RADIAL FLOW WITHOUT SWIRL BETWEEN PARALLEL DISCS WHEN THE FLOW IS COMPRESSIBLE AND SUBSONIC

by

P.S. Moller

Report 63-7

Mechanical Engineering Research Laboratories

McGill University

Supported under D.R.B. Grant Number 9551-12

Montreal April 1963

ACKNOWLEDGEMENTS

The author wishes to express his sincere gratitude to Dr. B.G. Newman for his guidance and advice in the course of this work.

Messrs. A. Gustavsen, E. Hansen and L.Vroomen are thanked for their assistance in the construction of the apparatus.

The work was financially supported by the Defence Research Board of Canada under DRB Grant No.9551-12.

SUMMARY

A combined experimental and theoretical study of radial compressible flow without swirl between parallel discs has been made when the fluid velocity is everywhere subsonic. It constitutes an extension of a previous analysis by the same author[1], wherein the flow was considered to be incompressible.

A similarity solution for the radial pressure distribution is shown to be possible only in special cases where certain terms in the equations of motion can be neglected. Approximate solutions are obtained for the laminar and the turbulent radial pressure distributions using an integral momentum method. Both theories agree well with experiment. The critical Reynolds number for reverse transition is found to be approximately the same as that for incompressible flow in radial channels and circular pipes.

CONTENTS

NOTATION

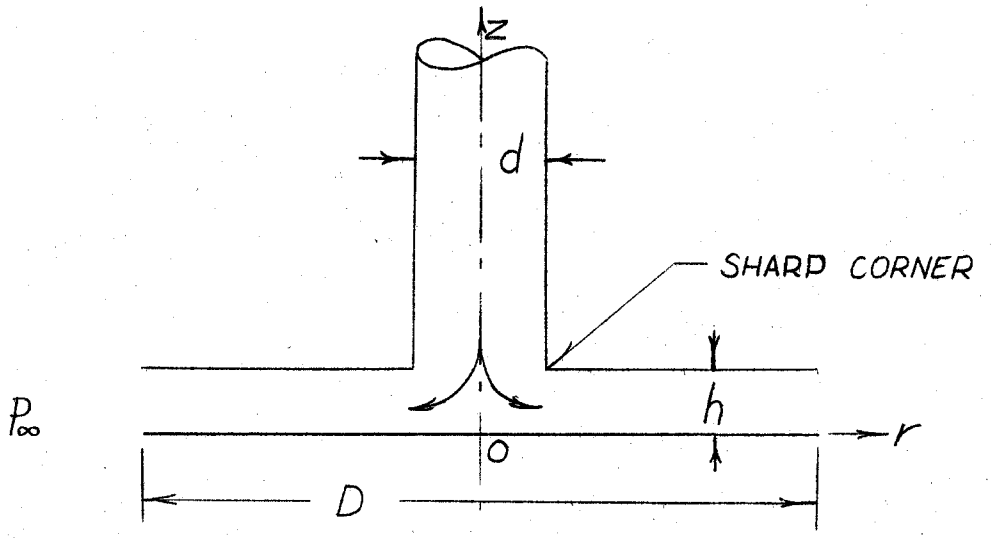

a - speed of sound = $\sqrt{\gamma RT}$

C_f - friction coefficient $\frac{\tau_o}{\frac{1}{2}\rho\bar{u}^2}$

d - inlet pipe diameter

D - channel diameter

h - channel height or width

m - empirical exponent entering the expression for turbulent skin friction

M - channel mass-flow

n - power-law exponent describing the turbulent velocity profile

p - static pressure on the channel wall (time mean when turbulent)

p_o - stagnation pressure at r = 0, z = 0

p_∞ - static pressure of surrounding fluid at rest

P - non-dimensional pressure = $\frac{p}{p_\infty}$

r - radial cylindrical co-ordinate measured from the centre-line of the inlet pipe

R - non-dimensional radius = $\frac{2r}{D}$

R_e - local channel Reynolds number based on the mean velocity and twice the channel width $\frac{M}{\pi r \mu}$

R_D - channel Reynolds number at exit = $\frac{2M}{\pi D \mu}$

T - temperature of fluid

u - time mean velocity in the radial direction

$\bar{u}$ - mean value of u across the channel at a particular radius

U_o - local maximum velocity in the centre of the channel

U_τ - skin friction velocity = $\sqrt{\frac{\tau_o}{\rho}}$

w - velocity in the z direction

z - axial co-ordinate measured normal to the back disc

α - empirical constant entering the wall shear-stress expression for turbulent flow

$\mathcal{R}$ - gas constant

ρ - density of fluid (time mean when turbulent)

ν - kinematic viscosity of fluid

μ - absolute viscosity of fluid

τ - radial shear-stress in planes perpendicular to oz

τ_o - wall shear-stress or skin friction

ξ - variable which accounts for small changes in the shape of the velocity profile in the radial direction

ψ - compressibility parameter = $\frac{\mu^2 \mathcal{R} T}{p_\infty{}^2 D^2} = \frac{1}{\gamma} \left(\frac{\mu a}{D p_\infty}\right)^2$

ϕ - constant introduced in equation (23)

γ - ratio of specific heats

$'$ - $\frac{d}{dz}$

$''$ - $\frac{d^2}{dz^2}$

1. INTRODUCTION

This paper describes an experimental and theoretical investigation into compressible radial flow between parallel circular discs. The flow which has radial symmetry is supplied without swirl through the centre of one of the discs and the fluid velocity is subsonic. In the experimental investigation the working fluid used was air.

This radial type of fluid motion is of particular interest in gas-bearings where the flow is dominated by friction as it moves radially outward. In this condition a positive gauge pressure exists between the discs which tends to hold them apart. The discs are then free to move relative to each other with a greatly reduced friction due to the inherently low viscosity of gases. The analysis in the present report is undertaken to develop equations describing this radial pressure distribution in order to improve air bearing design.

At sufficiently low Reynolds numbers, the flow in the radial channel is laminar. A creeping flow compressible solution predicting the radial pressure distribution under these conditions has been obtained by a number of investigators, e.g. (Gottwald [2], Weber [3], Licht and Fuller [4]). Deuker and Wojtech [5] and Gross [6] have obtained more complete solutions which includes the first order effects of the fluid inertia.

With increasing mass-flow, the Reynolds number at the inlet may exceed a critical value so that turbulent flow will exist for some distance downstream of the inlet corner. When the velocity, which decreases with increasing radius, has fallen sufficiently for the local Reynolds number to become sub-critical, a reverse transition from turbulent to laminar flow results, (Moller[1]). The phenomenon of reverse transition in other contexts has been studied by Sibulkin[7] and Sternberg[8].

If the mass-flow is increased still further the flow in the channel becomes fully turbulent and eventually the inertia terms will predominate over the viscous terms in determining the pressure distribution.

There seems to have been very little theoretical work done on radial turbulent flow other than the incompressible analysis carried out by Woolard[9], Welantz[10] and Moller[1].

In the present investigation the flow is examined for the existence of similarity solutions, with the result that certain limiting solutions are obtained. Approximate solutions, which include both inertia and viscous terms, are obtained for the radial pressure distribution when the flow is laminar or turbulent. Both solutions are based on the momentum integral equation together with a suitable expression for the shape of the velocity profile. In the turbulent case an approximate form for the pressure distribution is assumed so that the density gradient terms (due to compressibility) can be integrated.

2. DIMENSIONAL ANALYSIS

The flow is assumed to be subsonic at the channel inlet. Thus the fluid velocity will decrease rapidly in the radial direction due to increase of channel area, provided that $\frac{d}{D} \ll 1$. Kinetic temperature effects are therefore confined to a region near the inlet, and since in general the inlet fluid temperature is approximately equal to the ambient temperature, the flow is assumed to be isothermal. The isothermal condition is verified by experimental evidence obtained by a number of authors e.g. (Grinnell[11], and Comolet[12]).

The following parameters are therefore sufficient to define the flow for given inlet flow conditions:

h height or width of the channel

d diameter of inlet supply pipe

D diameter of channel

M mass-flow through inlet supply pipe

μ absolute viscosity of fluid

a speed of sound in fluid

p_∞ ambient pressure

γ ratio of specific heat

and entry boundary shape.

Thus the relevant criteria of similarity for this flow can be expressed non-dimensionally as:

γ, $\frac{h}{d}$, $\frac{D}{d}$, $\frac{M}{d\mu}$, $\frac{\mu a}{dp_\infty}$, entry boundary shape.

Downstream of the channel inlet the flow depends only on the total mass-flow coming into the channel and is independent of d and the entry boundary shape.

The pressure p at any radius r may be written non-dimensionally as:

$$\frac{p}{p_\infty} = f\left(\frac{h}{D}, \frac{M}{D\mu}, \frac{\mu a}{D p_\infty}, \frac{r}{D}, \gamma\right) \qquad .....(1)$$

for all entry shapes and values of $\frac{D}{d}$.

At sufficiently high Reynolds numbers, the parameter due to compressibility $\frac{\mu a}{D p_\infty}$ and the Reynolds number $\frac{M}{D\mu}$ could be combined to form a Mach number. However, in general when the flow is dominated by viscosity as in the present analysis, it is anticipated that the Reynolds number is an important independent parameter. This is confirmed by the detailed analysis which follows.

3. DETAILED THEORETICAL ANALYSIS

3.1 Similarity in Radial Channel Flow

The flow is first examined for similarity since such a condition would result in the simpliest possible complete solution to the equations of motion for the flow.

The following assumptions are made:

(i) The fluid velocity is everywhere subsonic

(ii) The flow is isothermal (refer to section 2)

(iii) The flow completely fills the channel and there is no back-flow

(iv) The flow is radially-symmetric and is free from swirl

(v) The fluid density is essentially constant across the channel

(vi) The density fluctuations, associated with turbulent compressible flow, can be neglected since the local Mach number is generally $<< 1$ (see section 2 and Lin[13])

With the above assumptions the equation of continuity for laminar or turbulent mean flow becomes:

$$\frac{1}{r\rho}\frac{\partial}{\partial r}(r\rho u) + \frac{\partial w}{\partial z} = 0 \qquad \ldots(2)$$

since p is independent of z.

A general expression for the velocity profile with similarity may be written

$$u = F(r)\, f(z) \qquad \ldots.(3)$$

Combining (2) and (3)

$$w = \frac{1}{r\rho}\frac{\partial}{\partial r}(\rho r F(r)) \int_o^z f(z)dz \quad \text{since } w = 0 \text{ at } z = 0$$

From the second boundary condition; $w = 0$ at $z = h$ and since M, the total mass-flow, is positive,

$$\int_o^h f(z)dz \neq 0$$

Thus
$$u = \frac{f(z)}{r\rho}$$
$$w = 0 \text{ everywhere} \qquad \ldots(4)$$

The equation of motion in the radial direction for both laminar and turbulent steady flow with $w = 0$ and μ = constant (isothermal flow), is:

$$u\frac{\partial u}{\partial r} + \frac{1}{r\rho}\frac{\partial}{\partial r}\overline{r\rho u'^2} + \frac{\partial}{\partial z}(\overline{u'w'}) = -\frac{1}{\rho}\frac{\partial p}{\partial r} + \nu\frac{\partial^2 u}{\partial z^2}$$
$$+ \nu\frac{4}{3}\left[\frac{\partial^2 u}{\partial r^2} + \frac{1}{r}\frac{\partial u}{\partial r} - \frac{u}{r^2}\right] \qquad \ldots(5)$$

Since $r \gg z$, $\left[\frac{\partial^2 u}{\partial r^2} + \frac{1}{r}\frac{\partial u}{\partial r} - \frac{u}{r^2}\right]$ can be neglected compared with $\frac{\partial^2 u}{\partial z^2}$

Assuming that the structure of the large eddies is also similar or self-preserving, $(\overline{u'w'})^{\frac{1}{2}}$ has the same form as (3)

Thus
$$\overline{u'w'} = \frac{g(z)}{r^2\rho^2} \qquad \ldots(6)$$

Neglecting $\frac{1}{r\rho}\frac{\partial}{\partial r}\overline{r\rho u'^2}$ as small when compared with $u\frac{\partial u}{\partial r}$ and

substituting for (4) and (6), equation (5) becomes:

$$f^2\left[1 + \frac{rd\rho}{\rho dr}\right] - rg' = r^3\rho \frac{dp}{dr} - \mu r^2 f'' \qquad \ldots(7)$$

which applies generally to laminar or turbulent flow.

From assumption (v), the equation of motion in the z direction becomes

$$p = \text{constant}$$

Equation (7) is true for all z and r. Therefore, from the assumption of similarity, it should split into independent equations in these variables. It is clear that in general this is impossible, except for special cases in which certain of the terms in the equation are negligibly small. The confined boundaries and the flow divergence in the radial channel make it unrealistic to assume that the pressure term could be neglected as small in general. Thus it must be combined with just one of the other three terms to obtain a special similarity solution.

Special Similarity Solutions:

Three cases are considered:

(i) Laminar creeping flow solution where the inertia and turbulent terms are neglected.

From equation (7)

$$r\rho \frac{dp}{dr} = \mu f'' = K_1$$

Substituting for $p = \rho \mathcal{R} T$, integrating and eliminating K_1 through continuity, the non-dimensional pressure for any value of r becomes:

$$\frac{p}{p_\infty} = \left[1 + 6R_D \left(\frac{\mathcal{R} T \mu^2}{D^2 p_\infty^2} \right) \left(\frac{1}{\frac{h}{D}} \right)^3 \ln \frac{D}{2r} \right]^{\frac{1}{2}} \qquad \ldots(8)$$

and the velocity distribution across the channel becomes:

$$\frac{u}{U_o} = 4 \left[\frac{z}{h} - \left(\frac{z}{h} \right)^2 \right]$$

It should be noted in passing that the channel Reynolds number $R_D = \frac{2M}{\pi D \mu}$ is formed using the effective hydraulic diameter (2h). This is a particularly useful dimension since it allows the Reynolds number for transition to be compared directly with the value for a circular pipe.

Equation (8) is the compressible creeping flow solution which has been obtained by a number of previous investigators.. ..(2), (3), (4). This laminar flow solution is expected to predict the radial pressure distribution accurately only when the ratio $\frac{\text{inertia force}}{\text{viscous force}} \sim R_e \left(\frac{h}{r} \right) \ll 1$ and $R_e <$ theoretical Reynolds number for reverse transition.

(ii) Inviscid Compressible Solution where the viscous and turbulent terms are neglected.

From equation (7)

$$\frac{1}{f^2} = \frac{1 + \frac{r}{p} \frac{dp}{dr}}{r^3 \rho \frac{dp}{dr}} = K_2$$

Substituting for $p = \rho RT$, integrating and eliminating K_2 through continuity the equation relating the non-dimensional pressure for any value of r becomes:

$$\frac{1}{8}\left[1 - \frac{\left(\frac{D}{2r}\right)^2}{\left(\frac{p}{p_\infty}\right)^2}\right] R_D^{\,2} \; \frac{1}{\left(\frac{h}{D}\right)^2} \left(\frac{\mu^2 \mathcal{R} T}{D^2 p_\infty^{\,2}}\right) = \ln \frac{p}{p_\infty} \qquad \ldots(10)$$

and the velocity distribution is uniform

$$\text{i.e. } \frac{u}{U_o} = 1.$$

The above equations may be expected to describe the main body of a turbulent flow in which $R_e\left(\frac{h}{r}\right) \gg 1$.

(ii) The combination of the turbulent term and the pressure term would yield a turbulent inviscid creeping flow solution, which has no practical significance in radial channel flow.

For turbulent flow an inviscid similarity solution might be possible when expressed in terms of the velocity defect, using U_o as datum. However, further examination of the momentum equation indicates that such a creeping flow solution is only possible for incompressible flow and for large $\frac{r}{h}$, that is when the flow approximates that in a two-dimensional channel. The validity of the velocity defect law in this case is, of course, well established.

3.2 Approximate Solutions for the Pressure Distribution Using the Integral Momentum Equation

3.2.1 Laminar Flow:

The use of an integral method to solve the radial channel flow equation may be expected to furnish fairly accurate results for a gross quantity such as the pressure distribution

An expression is assumed[1] which represents the velocity profile over half the channel. This expression differs by a small perturbation from the parabolic velocity distribution obtained for creeping flow.

$$\frac{u}{U_o} = 4\frac{z}{h}\left(1 - \frac{z}{h}\right) + \xi\frac{z}{h}\left(1 - 2\frac{z}{h}\right)^3 \qquad \ldots(11)$$

which satisfies the boundary conditions

$$u = 0 \quad \text{at} \quad z = 0$$

$$\frac{\partial u}{\partial z} = 0 \quad \text{at} \quad z = \frac{h}{2}$$

The momentum equation for radial flow, considering an annular control volume, is:

$$-phdr + \frac{\partial}{\partial r}(prh)dr + 2\tau_o r dr = -\frac{\partial}{\partial r}\left[2r\int_o^{\frac{h}{2}} \rho u^2 dz\right]dr \qquad \ldots(12)$$

and the first compatibility at the wall is:

$$\frac{dp}{dr} = \left(\frac{\partial \tau}{\partial z}\right)_o \qquad \ldots(13)$$

Moller[1] has noted the insensitivity of the inertia term to changes in the shape of the velocity profile for

incompressible flow. In the present analysis it is therefore assumed that the ξ term can be neglected when considering the integral inertia term but <u>not</u> when considering the skin friction term.

Substituting for u and integrating across the channel, equation (12) becomes:

$$\frac{8}{15}\rho h U_o \frac{dU_o}{dr} = -\frac{dp}{dr} h - 2\tau_o \qquad \ldots(14)$$

From (11) and (13)

$$\xi = -\frac{2}{3}\left[1 + \frac{dp}{dr}\frac{h^2}{\mu U_o}\right]$$

From the conservation of mass-flow

$$U_o = \frac{M}{2\pi r h \rho \left(\frac{2}{3} + \frac{\xi}{40}\right)}$$

Since $|\xi| \ll 1$ for a flow dominated by viscosity

$$U_o \backsimeq \frac{3M}{4\pi r h \rho}$$

The wall shear-stress from (11) is:

$$\tau_o = \left(\mu \frac{\partial u}{\partial z}\right)_o = \frac{\mu U_o}{h}\left[4 + \xi\right]$$

By substituting for τ_o and U_o in equation (14), putting $p = \rho \mathcal{R} T$, $R = \frac{2r}{D}$ and $P = \frac{p}{p_\infty}$, and then integrating between the radius R where the pressure is P and R = 1 where P = 1, the following equation for the pressure distribution is obtained.

$$P = \left\{ 1 + 6R_D\psi \frac{1}{\left(\frac{h}{D}\right)^3} \ln\frac{1}{R} - \frac{9}{25} R_D^2\psi \frac{1}{\left(\frac{h}{D}\right)^2} \left[\left(\left(\frac{1}{R}\right)^2 - 1 \right) + 2 \int_P^1 \frac{1}{R^2} \frac{dP}{P} \right] \right\}^{\frac{1}{2}} \quad \ldots(15)$$

Viscous Term — Area Term — Density Gradient Term

where $R_D = \frac{2M}{\pi D\mu}$ and $\psi = \frac{\mu^2 \mathcal{R} T}{p_\infty^2 D^2}$

Due to its particular form the density gradient term cannot be integrated explicitly. It might be presupposed however that in laminar flow the density gradient term is small relative to the dominant viscous term. To examine this a realistic range of the variables was considered and the magnitude of the density gradient term was ascertained relative to the viscous term by using the pressure gradient as determined from equation (15) with the density gradient term neglected. The range chosen was

$$0.1 < R < 0.9$$

$$0.0001 < \frac{h}{D} < 0.001$$

$$0.1 < \frac{d}{D} < 0.5$$

A limiting Reynolds number $\frac{2M}{\pi D\mu} = R_D \frac{D}{d} < 2000$ was assumed.

This is found to approximate the critical Reynolds number at which the flow would become turbulent at the channel inlet. A fifth limit set was that $\frac{p_o}{p} \leqslant 10$. which in fact imposes a limit on $R_D \frac{D}{d}$ in certain cases.

The largest value of the density gradient term was 4%

of the viscous term at $\frac{h}{D} = 0.0001$, $\frac{d}{D} = 0.5$, $R = 0.9$ and $\frac{p_o}{p_\infty} = 10$. In this extreme case the neglect of the density gradient term produced an error of only 2% in the local pressure. It is assumed therefore, that the density gradient term can usually be neglected without introducing a significant error in the final result.

Thus the equation for the radial pressure distribution for compressible laminar flow is:

$$\frac{p}{p_\infty} = \left\{1 + 6R_D\psi \frac{1}{(\frac{h}{D})^3} \ln \frac{D}{2r} - \frac{9}{25} R_D^2 \psi \frac{1}{(\frac{h}{D})^2} \left[(\frac{D}{2r})^2 - 1\right]\right\}^{\frac{1}{2}} \quad \ldots(16)$$

Neglecting the inertia term in the above equation gives the laminar, compressible creeping flow solution, (equation (8)).

Expanding the R.H.S. of equation (16) in a binomial series, the first two terms yield the incompressible laminar flow solution previously obtained by Moller[1].

$$\frac{p}{p_\infty} = 1 + 3R_D\psi \frac{1}{(\frac{h}{D})^3} \ln \frac{D}{2r} - \frac{9}{50} R_D^2 \psi \frac{1}{(\frac{h}{D})^2} \left[(\frac{D}{2r})^2 - 1\right] \quad \ldots(17)$$

3.2.2 Turbulent Flow

It is assumed that mean velocity distribution over half the channel is given by a power-law.

$$\frac{u}{U_o} = \left[\frac{z}{\frac{h}{2}}\right]^{\frac{1}{n}} \quad \ldots(18)$$

where n is independent of r.

This assumption implies that the velocity profiles are similar. Although this is not strictly correct, the associated inertia term is relatively insensitive to the choice of n[1].

Substituting for u and integrating across the channel, the momentum equation for an annular control volume, equation (12), becomes:

$$\frac{n}{n+2}\left(\rho h \frac{dU_o}{dr} U_o\right) = - h \frac{dp}{dr} - 2\tau_o \qquad \ldots(19)$$

Keenan and Neumann[14] have shown that the incompressible friction coefficient for turbulent channel flow applies well for compressible flow when it is related to the local Reynolds number R_e, computed using the mean temperature across the channel. Therefore, consistent with the power-law assumption and previous work with incompressible flow

$$C_f = \frac{\tau_o}{\frac{1}{2}\rho\bar{u}^2} = \frac{\alpha}{(R_e)^{\frac{1}{m}}} = \frac{.079}{(R_e)^{\frac{1}{4}}} \qquad \ldots(20)$$

where $4000 < R_e < 200{,}000$

α and m are taken from experimental work by Nikuradse[15], Schiller[16] and Moller[1] for ducts of various configurations.

Relating m to n through equation (18) and $U_\tau = \left(\frac{\tau_o}{\rho}\right)^{\frac{1}{2}}$ gives $\frac{u}{U_\tau} \propto \left(\frac{zU\tau\rho}{\mu}\right)^{\frac{1}{2m-1}} \left(\frac{h}{z}\right)^{\frac{1}{2m-1} - \frac{1}{n}}$

Thus if the law of the wall holds for a certain distance from the wall, $\frac{u}{U_\tau} = F\left(\frac{zU\tau\rho}{\mu}\right)$

and $n = 2m - 1$ $\qquad \ldots(21)$

By substituting for τ_o and U_o in equation (19) and putting $p = \rho \mathcal{R} T$, $R = \frac{2r}{D}$, $P = \frac{p}{p_\infty}$ and then integrating from the radius R where the pressure is P to R = 1 where P = 1, the following equation for the pressure distribution is obtained:

$$P = \left\{ 1 + .02635\, R_D^{\frac{7}{4}} \psi \frac{1}{(\frac{h}{D})^3} \left(\frac{1}{R^{\frac{3}{4}}} - 1 \right) - \frac{16}{63} R_D^2 \psi \frac{1}{(\frac{h}{D})^2} \left[\left((\frac{1}{R})^2 - 1 \right) + 2 \int_P^1 \frac{1}{R^2} \frac{dP}{P} \right] \right\}^{\frac{1}{2}} \quad \ldots(22)$$

where $R_D = \frac{2M}{\pi D \mu}$ and $\psi = \frac{\mu^2 \mathcal{R} T}{p_\infty^2 D^2}$

As in the laminar solution, the density gradient term in the above equation cannot be integrated explicitly. In radial turbulent flow this term is small but generally cannot be neglected. Preliminary experimental results have shown that a good approximation for the turbulent pressure distribution far from the inlet corner is:

$$P = e^{\frac{\phi}{2}(1 - R)} \quad \ldots(23)$$

where ϕ is a constant

This particular pressure distribution is chosen for convenience in the evaluation of the density gradient term.

Using equation (23) to integrate the density gradient term, equation (22) becomes:

$$\frac{p}{p_\infty} = \left\{ 1 + .02635\, R_D^{\frac{7}{4}} \psi \frac{1}{(\frac{h}{D})^3} \left[(\frac{D}{2r})^{\frac{3}{4}} - 1 \right] - \frac{16}{63} R_D^2 \psi \frac{1}{(\frac{h}{D})^2} \left[(\frac{D}{2r})^2 - 1) - \phi(\frac{D}{2r} - 1) \right] \right\}^{\frac{1}{2}} \quad \ldots(24)$$

where ϕ is given by equations (25)

ϕ is evaluated by matching the assumed pressure distribution (equation (23)) and equation (24) at an arbitrarily chosen radius provided that the flow is independent of the channel inlet conditions.

In the present analysis the radius $r = \frac{D}{4}$ is chosen and thus

$$\phi = 2\ln \left[A - B(1 - \frac{\phi}{3}) \right]$$

where

$$A = 1 + \frac{.01795\, R_D^{\frac{7}{4}} \psi}{(\frac{h}{D})^3} \quad \ldots(25)$$

$$B = \frac{48}{63} \frac{R_D^2 \psi}{(\frac{h}{D})^2}$$

An exact value for ϕ may be obtained by successive approximations. In practice it is usually sufficient to proceed to the second approximation only.

Neglecting the density gradient term in equation (24) and expanding the R.H.S. in a binomial series, the first two terms yield the incompressible turbulent solution previously obtained by Moller[1].

$$\frac{p}{p_\infty} = 1 + .0132\, R_D^{\frac{7}{4}} \psi \frac{1}{(\frac{h}{D})^3} \left[(\frac{D}{2r})^{\frac{3}{4}} - 1 \right] - \frac{8}{63} R_D^2 \frac{1}{(\frac{h}{D})^2} \psi \left[(\frac{D}{2r})^2 - 1 \right] \quad \ldots(26)$$

4. DETAILS OF EXPERIMENTAL INVESTIGATION

The experimental apparatus which was used to investigate the radial channel flow is shown in figure 7 and described in the Appendix. A comprehensive investigation was made for unchoked laminar and turbulent flow where the effects of changing the Reynolds number R_D and channel width $\frac{h}{D}$ were determined.

To make the results as specific as possible, the inlet pipe was made sufficiently long and straight for fully developed, swirl free, symmetric pipe flow to exist at the entrance to the radial channel, and the corner between the inlet pipe and the channel was made as sharp as possible.

An experimental investigation was also undertaken near the anticipated Reynolds number for transition so that the laminar and turbulent theories could be checked at their expected limit of applicability, and so that the critical Reynolds number for reverse transition could be determined.

5. DISCUSSION OF EXPERIMENTAL RESULTS AND COMPARISON WITH THEORY.

5.1 General

It is noted that the air enters through the back disc and impinges upon the front disc.

The radial symmetry was checked by measuring the static gauge pressures along two mutually-perpendicular diameters and these were found to be in agreement to an accuracy of better than 0.4 per cent. Furthermore a continual check on the radial symmetry was maintained since the pressures presented in the various figures were measured along two radial lines perpendicular to each other.

The pressure distribution was identical on both disc faces except very near the inlet, where the pressure on the front disc was higher (figure 5.) All pressures quoted on the figures are for the front disc unless otherwise noted.

5.2 Laminar Pressure Distribution

When the maximum local Reynolds number R_e, which occurs at the channel entry, is sub-critical, laminar flow will exist throughout the channel. Figure 1 gives the pressure distribution for various channel Reynolds numbers and radial positions r. The results have been plotted non-dimensionally in accordance with equation (16). It can be seen that agreement between experiment and theory is generally very good, the greatest departures being

near the channel inlet where entrance conditions would be expected to become important. The creeping flow solution (equation (8)) is also plotted in figure 1, and at the lowest Reynolds number (R_D = 83.3), this solution satisfactorily predicts the radial pressure distribution. However, the creeping flow solution is clearly less accurate than equation (16) at the highest Reynolds number (R_D = 400).

Figure 2 shows a second comparison with equation (16) for various channel widths h at a constant Reynolds number R_D. The incompressible solution (equation (17)) is also plotted in one case.

5.3 Turbulent Pressure Distribution

If the channel exit Reynolds number is high enough, (R_D greater than about 2000), the flow is turbulent throughout the channel.

Figure 3 gives the pressure distribution for various channel Reynolds numbers and radial positions r at a constant channel width h. The results have been plotted non-dimensionally in accordance with equation (24). A second approximation only was used to determine the constant ϕ. The agreement with theory as r decreases is good up to a point near the channel inlet where the assumed exponential pressure distribution (equation (23)) used to integrate the density gradient term, becomes inaccurate.

The disagreement between theory and experiment may also be attributed to the effects of the entrance conditions on the flow downstream of the channel inlet. Since the entrance corner is sharp a certain degree of flow separation from the back disc must be present, and this leads to lower experimental pressures.

Figure 4 shows the effect of varying the channel width at a constant Reynolds number. Certain experimental points for which $\frac{p}{p_\infty}$ is < 1 are ommitted from the figure. It can be seen, therefore, that agreement between theory and experiment is best when the channel width is small. Under these conditions, the assumed exponential pressure distribution is most accurate, and entrance conditions have the least effect on the flow downstream of the channel inlet.

The effect of using a second approximation for ϕ, rather than the exact value from equation (25), is shown in figure 5, and the difference is seen to be small. The experimental pressures for both the front and the back disc have been plotted. It is noted that near the channel inlet, the experimental pressure distribution for the back disc is lower than that for the front disc. Some value falling between those for the front and back discs would be the most representative of the mean flow pressure distribution and would give a slightly better agreement between theory and experiment than that shown in the figures. The incompressible pressure distribution as given by equation (26) is also shown for comparison.

5.4 Transition

The critical Reynolds number (R_e) for reverse transition is determined from the measured pressure distribution by considering the variation of pressure with the local Reynolds number (R_e) at a specific radius. Figure 6 shows the non-dimensional pressure $\frac{p}{p_\infty}$ for three values of $\frac{r}{D}$, plotted against the local R_e. Transition occurs at a critical R_e of approximately 2000 in all three cases and is thus in agreement with the critical Reynolds number for incompressible radial flow[1]. Since reverse transition is occurring, this Reynolds number must be the lowest critical Reynolds number for conventional transition from laminar to turbulent flow.

It is expected that the previous explanation given by Moller[1] for the phenomenon of reverse transition in incompressible flow is also valid in the present compressible case.

6. CONCLUSIONS

For compressible but subsonic gas-flow, without swirl, through a radial channel, it is concluded that:

(i) The radial pressure distribution for laminar flow, sufficiently far downstream of the channel entrance, may be predicted with good accuracy by an approximate theory assuming isothermal conditions. This theory makes use of the integral momentum equation together with the first compatibility condition at the wall. A suitable form for the velocity profile is assumed which allows it to vary slightly from the parabolic shape appropriate for creeping flow.

(ii) The pressure distribution for turbulent flow may also be predicted by a similar theory. This solution again makes use of the integral momentum equation, in conjunction with a power-law expression for the velocity profile and an assumed form for the pressure distribution which allows the implicit density gradient term to be integrated.

(iii) The critical Reynolds number (based on the mean velocity and the hydraulic diameter) is approximately 2000 for reverse transition from turbulent to laminar flow and is therefore similar to the critical Reynolds number for incompressible flow in radial channels and circular pipes when the entrance flow is highly disturbed.

7. APPENDIX

Apparatus and Experimental Procedure:

The apparatus shown in figure 7 was designed to produce swirl-free, compressible, laminar or turbulent radial channel flow with fully developed pipe flow at the entrance. Air was supplied by three reciprocating compressors connected in parallel to a common reservoir and supply line. All the compressors were powered by constant-speed three phase-motors, one 40 H.P. and two 15 H.P. The air was filtered at each individual compressor intake, cooled by a common water after-cooler and passed through a water separator. The maximum mass-flow that could be supplied was 0.3 lb/sec. Pipes 2 ins. in diameter connected the compressor room with the Aerodynamics Laboratory where the air pressure was regulated to an accuracy of $\pm$ 1 psi. Near the apparatus a reservoir was located to damp out any pressure fluctuations in the supply line. Upon leaving the reservoir, the air passed through an orifice plate and a large gate valve. These served to meter and control the flow at high mass-flows. The air then travelled down a length of straight drawn aluminium pipe 2 ins. in diameter and 150 pipe diameter long before entering the radial channel. To obtain medium and low mass-flows, the air was redirected around the gate valve and through an additional instrument pressure regulator of $\pm$ .05 psi. accuracy. Depending on the

mass-flow requirements, the air then passed through one of three flow rotameters (capacity .025 - 25 c.f.m.) which has an accuracy of ± 1% of maximum flow. The rotatmeters were generally operated at or near their maximum capacity so that the flow was measured with the least error.

The radial channel was formed by two 1.250 inch thick machined steel discs 10 ins. in diameter. In the back disc there was a hole 2 ins in diameter through which the air entered the channel from the inlet supply pipe. The back disc was mounted rigidly on a heavy steel framework, and the front disc moved on three threaded steel rods. Three dial gauges with 0.0001 inch graduations were mounted on the rigid frame and rode against the front disc so that the channel width could be quickly adjusted to an accuracy of 0.0001 inch or better. In order to obtain consistent experimental results, it was necessary to set the channel to within ± 0.000025 inch tolerance at the small channel widths which were used to investigate the laminar flow regime. This accuracy was achieved by using high quality feeler gauges (specially measured to within this tolerance) at three points around the channel circumference where the channels were tightly clamped together with C-clamps. The steel discs were ground to a nominal accuracy of 10 micro-inches and then machine lapped face to face with a very fine grade of grinding powder such as

is used for preparing metallurgical specimens. After 12 hours of continuous lapping in this way the resulting surface proved very satisfactory.

The front disc was pressure tapped with holes 0.020 ins. in diameter at 0.2 inch radial increments along two perpendicular radii. In this way a continuous check on the radial symmetry was provided. The back disc was pressure tapped at 0.4 inch radial increments. A number of additional pressure taps were drilled in both discs in order to obtain a more complete check on the radial symmetry. The radial static pressures were recorded by means of a specially designed pressure recording instrument constructed by the McGill University Instrument Laboratory[17]. The pressures were first passed into a 48-port Scani-valve which scanned the pressure taps at the rate of one per second. The Scani-valve distributed the individual pressures through a (0 - 50 psig.) bi-directional pressure transducer whose output was passed through a variable gain amplifier and then recorded on a self-balancing potentiometer.

REFERENCES

1. Moller, P.S. — Radial Flow Without Swirl Between Parallel Discs. Aeronautical Quarterly, (May 1963).

2. Gottwald, F. — Investigations on Bearing Devices with Small Friction. Foreign Document Evaluation Branch, Ordinance Research and Development Centre, Aberdeen Proving Ground, Maryland. Report No.15. (April 1946).

3. Weber, R.R. — The Analysis and Design of Hydrodynamics Gas Bearings. North American Aviation Inc., Aerophysics Lab. Report AL-699 (1949).

4. Licht, L. and Fuller, D.D. — A Preliminary Investigation of an Air-Lubricated Hydrostatic Thrust Bearing. A.S.M.E., Paper No. 54-LUB-18, (1954).

5. Deuker, E.A. and Wojtech, H. — Ecoulement Radial d'un Fluide Visqueux Entre Deux Disques tres Rapproaches; Theorie du Palies a Air. Revue Generale de L'Hydraulique, Vol 17, p.227-234, 285-294 (1953)

6. Gross, W.A. — Gas Film Lubrication. John Wiley and Sons Inc., p.268-269. (1962)

7. Sibulkin, M. — Transition from Turbulent to Laminar Pipe Flow. The Physics of Fluids, Vol.5, No.3 (March 1962)

8. Sternberg, J. — The Transition from Turbulent to Laminar Pipe Flow. B.R.L. Report 906, Ballistic Research Laboratories, Aberdeen Proving Ground, Maryland. (1954)

9. Woolard, H.W. — A Study of the Flow in a Narrowly-Spaced Radial Diffuser. Master of Science Thesis, Graduate School of the University of Buffalo, New York. (1954).

10. Welantz, L.F. — A Suction Device Using Air Under Pressure. Journal of Applied Mechanics. Trans. A.S.M.E., Vol. 78, p.269. (June 1956).

11. Grinnell, S.K. — Flow of a Compressible Fluid in a Thin Passage. Trans. A.S.M.E., Vol.78, p.765-771 (1956).

12. Comolet, R. — Ecoulement d'un Fluide Entre Deux Plans Paralleles, Contribution a l'Etude des Butees d'Air. Pub. Sci. et Techn. Ministere l'Air, No. 334. (1957).

13. Lin, C.C. — Turbulent Flows and Heat Transfer. Princeton University Press, p.89-107 (1959).

14. Keenan, J.H. and Neumann, E.P. — Measurements of Friction in a Pipe for Subsonic and Supersonic Flow of Air. Journal of Applied Mechanics, Paper No. A-91. (June 1946).

15. Nikuradse, J. — Turbulente Strömung in nicht kreisformigen Rohren. Ingenieur - Archiv. Vol.1, p.306, (1930).

16. Schiller, L. — Uberden Strömungswiderstand von Rohren verschiedenen Querschnitts und Rauhig keitsgrades. ZAMM, Vol.3, p.2. (1923).

17. Vroomen, L.J. — The Pressure Transducer Rack. Memo. 62-6, McGill University (1962).

FIG. 1

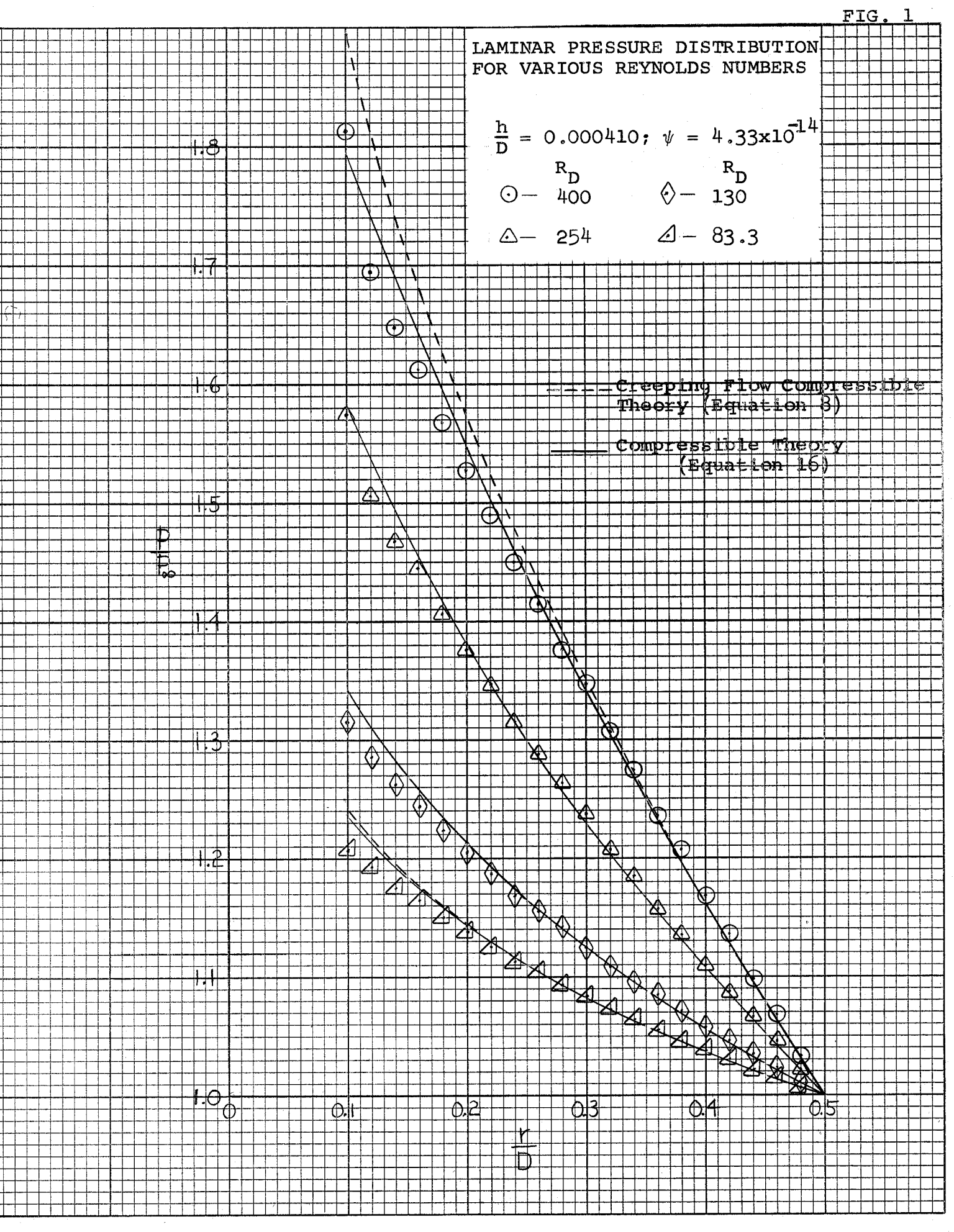
LAMINAR PRESSURE DISTRIBUTION FOR VARIOUS REYNOLDS NUMBERS
h/D = 0.000410; ψ = 4.33x10^-14
R_D
⊙ — 400
△ — 254
R_D
◇ — 130
◿ — 83.3
Creeping Flow Compressible Theory (Equation 8)
Compressible Theory (Equation 16)
P/P∞
r/D
1.8
1.7
1.6
1.5
1.4
1.3
1.2
1.1
1.0
0
0.1
0.2
0.3
0.4
0.5

FIG. 2

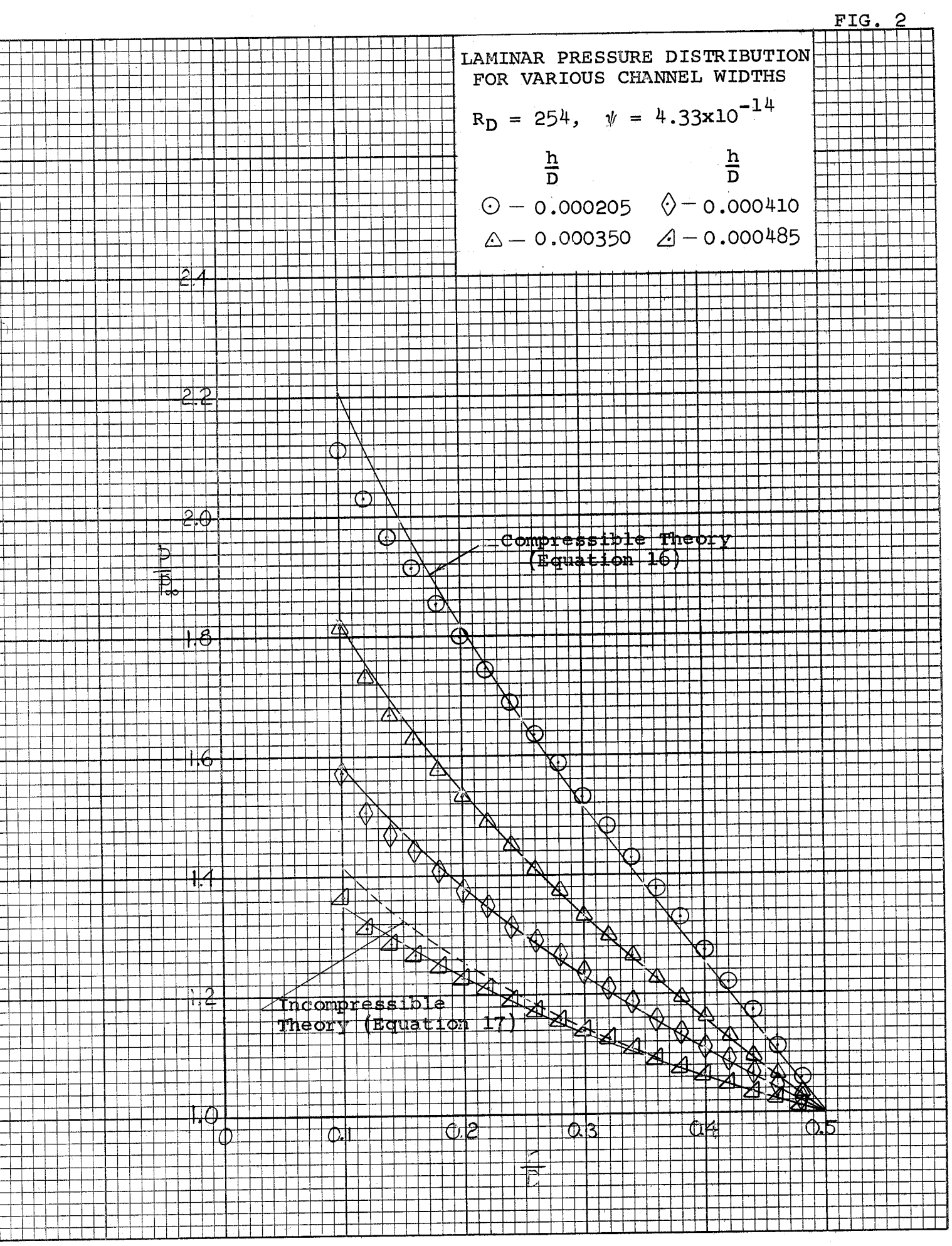
LAMINAR PRESSURE DISTRIBUTION
FOR VARIOUS CHANNEL WIDTHS
$R_D = 254$, $\psi = 4.33 \times 10^{-14}$
$\frac{h}{D}$
⊙ — 0.000205
△ — 0.000350
$\frac{h}{D}$
◇ — 0.000410
◿ — 0.000485
Compressible Theory
(Equation 16)
Incompressible
Theory (Equation 17)
$\frac{p}{p_\infty}$
2.4
2.2
2.0
1.8
1.6
1.4
1.2
1.0
0
0.1
0.2
0.3
0.4
0.5
$\frac{x}{L}$

FIG. 3

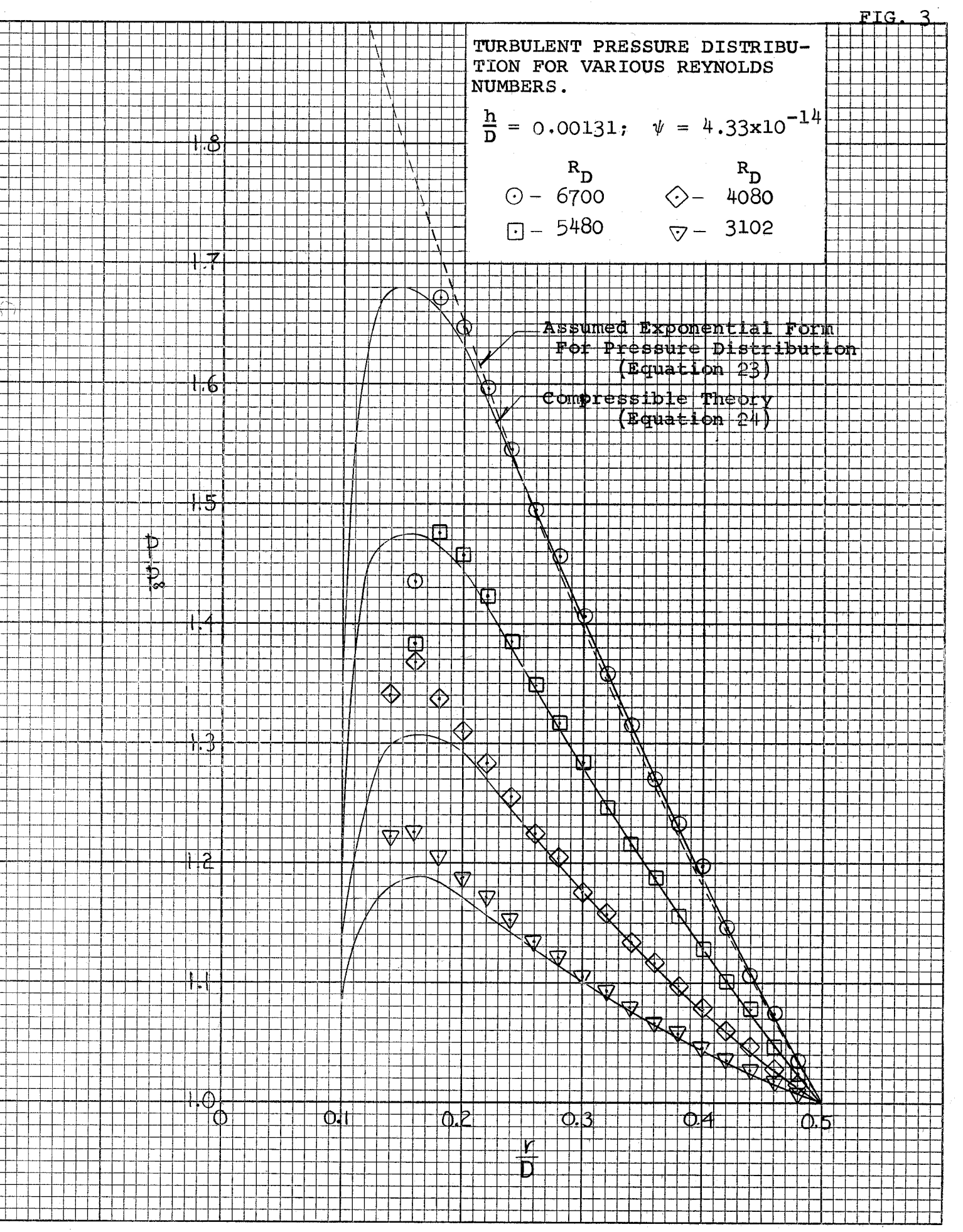
TURBULENT PRESSURE DISTRIBUTION FOR VARIOUS REYNOLDS NUMBERS.
h/D = 0.00131; ψ = 4.33x10^-14
R_D
⊙ - 6700
⊡ - 5480
R_D
◇ - 4080
▽ - 3102
Assumed Exponential Form For Pressure Distribution (Equation 23)
Compressible Theory (Equation 24)
p/p∞
1.8
1.7
1.6
1.5
1.4
1.3
1.2
1.1
1.0
0
0.1
0.2
0.3
0.4
0.5
r/D

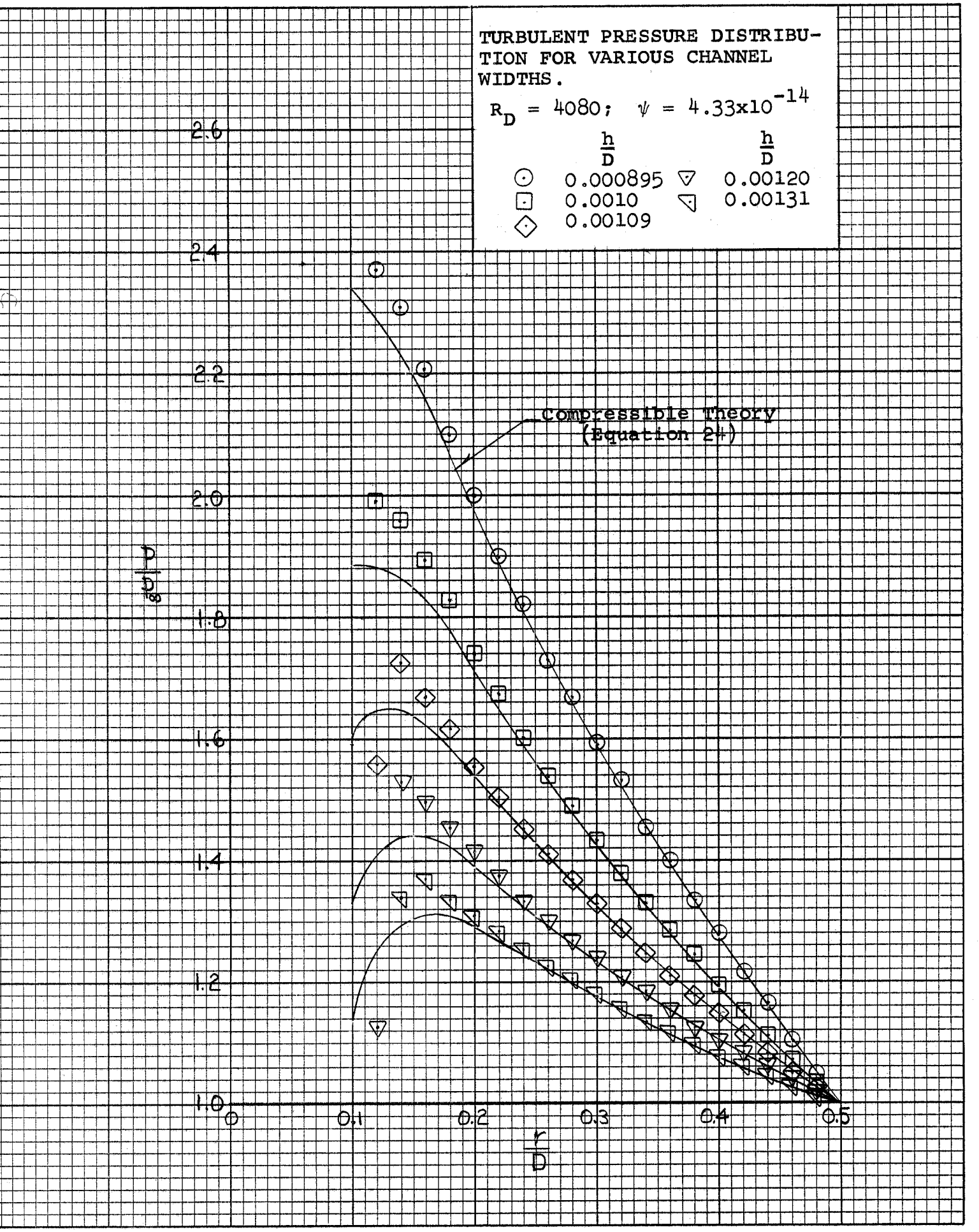
TURBULENT PRESSURE DISTRIBUTION FOR VARIOUS CHANNEL WIDTHS.
R_D = 4080; $\psi = 4.33 \times 10^{-14}$
h/D
0.000895
0.0010
0.00109
0.00120
0.00131
Compressible Theory (Equation 24)
P/P∞
r/D
2.6
2.4
2.2
2.0
1.8
1.6
1.4
1.2
1.0
0
0.1
0.2
0.3
0.4
0.5

FIG. 5

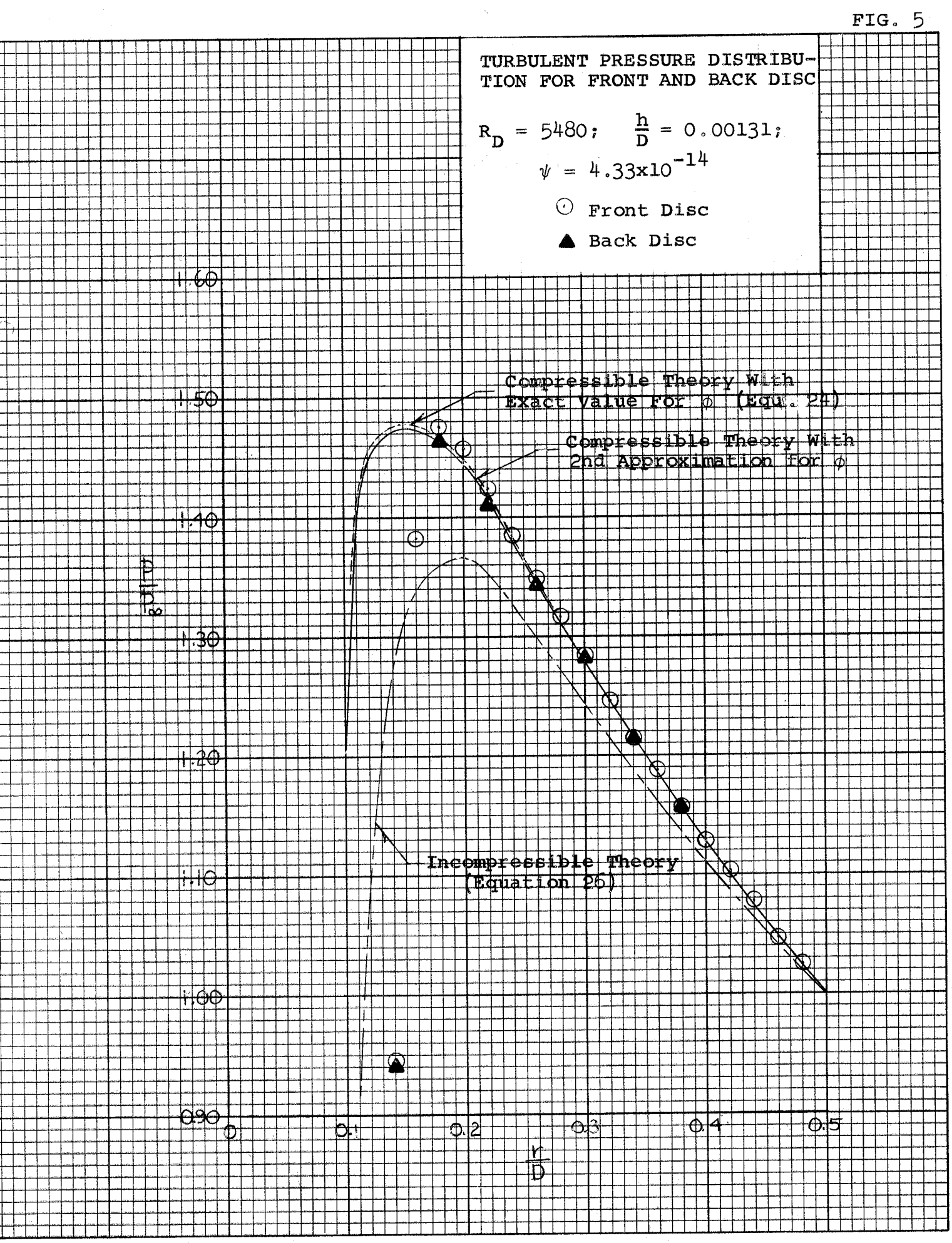
TURBULENT PRESSURE DISTRIBUTION FOR FRONT AND BACK DISC
R_D = 5480; $\frac{h}{D}$ = 0.00131;
$\psi = 4.33 \times 10^{-14}$
Front Disc
Back Disc
Compressible Theory With Exact Value For ϕ (Equ. 24)
Compressible Theory With 2nd Approximation for ϕ
Incompressible Theory (Equation 26)
$\frac{p}{p_\infty}$
1.60
1.50
1.40
1.30
1.20
1.10
1.00
0.90
0
0.1
0.2
0.3
0.4
0.5
$\frac{r}{D}$

FIG. 6

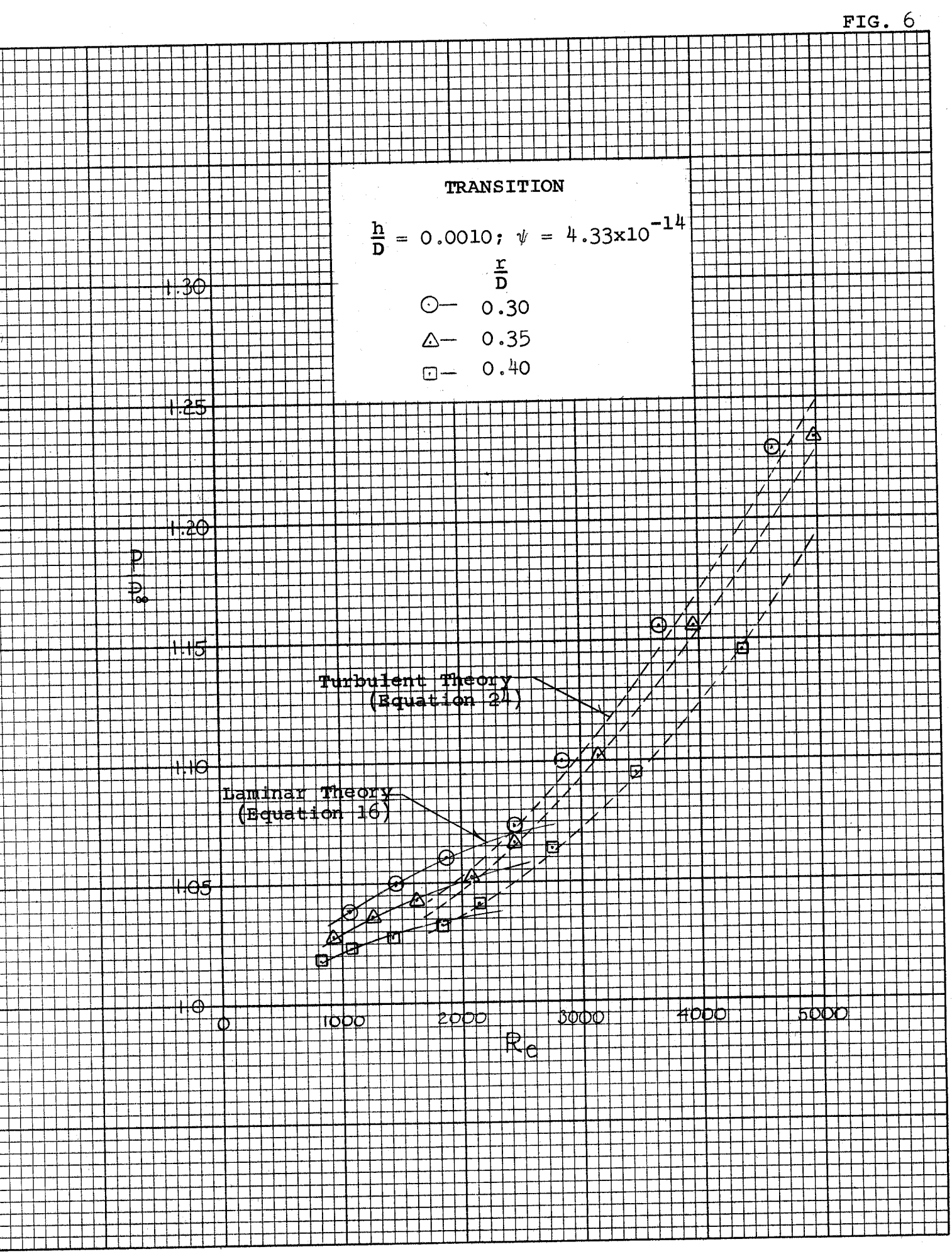
TRANSITION
h/D = 0.0010; ψ = 4.33x10^-14
r/D
0.30
0.35
0.40
1.30
1.25
1.20
1.15
1.10
1.05
1.0
P/P∞
Turbulent Theory
(Equation 24)
Laminar Theory
(Equation 16)
0
1000
2000
3000
4000
5000
Re

FIG.7

GENERAL VIEW OF EXPERIMENTAL APPARATUS

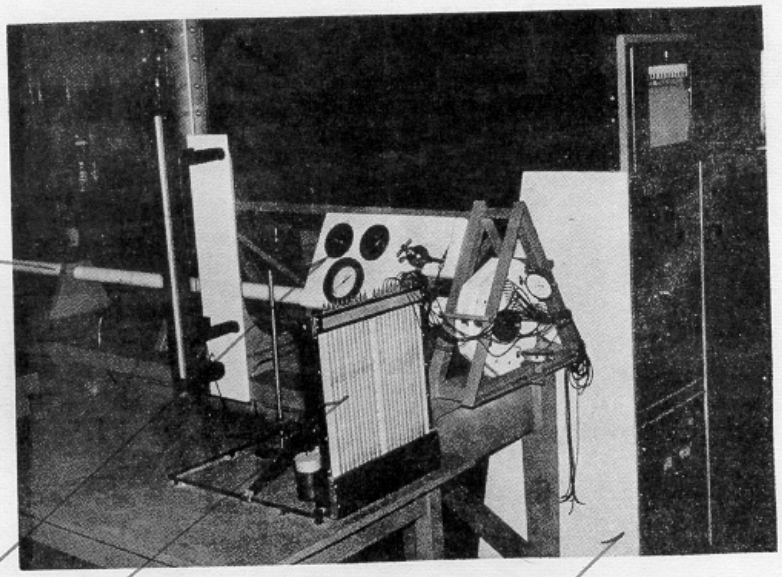

DETAILED VIEW OF RADIAL CHANNEL